

High sensitivity gas spectroscopy of porous, highly scattering solids

Tomas Svensson,^{1,*} Mats Andersson,¹ Lars Rippe,¹ Jonas Johansson,² Staffan Folestad,² and Stefan Andersson-Engels¹

¹Department of Physics, Lund University, SE-221 00 Lund, Sweden

²Astra Zeneca Research and Development, SE-431 83 Mölndal, Sweden

*Corresponding author: tomas.svensson@fysik.lth.se

Received October 23, 2007; revised November 20, 2007; accepted November 20, 2007; posted November 29, 2007 (Doc. ID 88933); published December 21, 2007

We present minimalistic and cost-efficient instrumentation employing tunable diode laser gas spectroscopy for the characterization of porous and highly scattering solids. The sensitivity reaches 3×10^{-6} (absorption fraction), and the improvement with respect to previous work in this field is a factor of 10. We also provide the first characterization of the interference phenomenon encountered in high-resolution spectroscopy of turbid samples. Revealing that severe optical interference originates from the samples, we discuss important implications for system design. In addition, we introduce tracking coils and sample rotation as new and efficient tools for interference suppression. The great value of the approach is illustrated in an application addressing structural properties of pharmaceutical materials. © 2007 Optical Society of America

OCIS codes: 300.6320, 120.6200, 290.4210, 170.7050, 170.5280, 120.4290.

High-resolution diode laser absorption spectroscopy (TDLAS) is a well established tool for selective and sensitive gas analysis and has proved its value in many areas of science, as well as in industrial applications [1,2]. The sensitivity of the technique is often improved by employing various noise reduction schemes, such as wavelength modulation spectroscopy (WMS) [3,4]. Since 2001, TDLAS and WMS have also been used for the sensing of gases dispersed within highly scattering media [5]. This approach, often referred to as gas in scattering media absorption spectroscopy (GASMAS), has since then been successfully used for the characterization of various materials, such as polystyrene foam [5,6], wood [7], fruit [8], biological tissue [9], and pharmaceutical solids [10]. However, GASMAS experiments suffer from a much lower sensitivity than the traditional use of TDLAS. By traditional use, we refer to setups with well-defined beam lines together with known and controllable interaction length (often using gas cells). In such a setup, sensitivities are often in the 10^{-7} range. In contrast, measurements of gas content in highly scattering solid samples involve dealing with severe backscattering, heavy attenuation, diffuse light, and uncontrollable and unknown interaction lengths. Sensitivities better than $\sim 5 \times 10^{-5}$ have never been reported until now. In the case of oxygen sensing at ~ 760 nm, an absorption fraction of 5×10^{-5} corresponds to more than a 1 mm path length in ambient air (1 mm L_{eq}). It should also be noted that these results have been achieved by imposing vibrations on the experimental setup (averaging out interference fringes). However, limited effort has been directed toward the understanding of the limitations in GASMAS.

In this Letter we have focused on understanding and restraining the negative effects of multiple scattering and have obtained a tenfold increase in GASMAS sensitivity in this way, reaching down to absorption fractions of 3×10^{-6} (a 1σ measure at 60 s

acquisition time, see Figs. 3 and 4). In addition, this is the first detailed characterization of GASMAS performance, as well as the first investigation of the optical interference phenomena that limits measurement quality. Our findings have important implications for the design of GASMAS instrumentation. Finally, the gained sensitivity is sufficient to fully match the needs in most applications, and thus makes the technique very attractive.

We employ a minimalistic, single-beam WMS-TDLAS instrumentation based on oxygen sensing with a vertical-cavity surface-emitting laser (VCSEL). The instrumentation is schematically described in Fig. 1. Briefly, a 0.3 mW VCSEL (V-763-OXY-MTE, Laser Components) is wavelength tuned over one of the absorption lines in the R branch of molecular oxygen [R9Q10, 760.654 nm vacuum wavelength, peak absorption coefficient $\mu_a = 2.83 \times 10^{-5} \text{ mm}^{-1}$ in ambient air, according to high-resolution transmission molecular absorption database (HITRAN)]. The modulation signal is created by an arbitrary waveform generator (AWG) (CH-3150, Exacq Technologies) running at 19.3536 MS/s, and

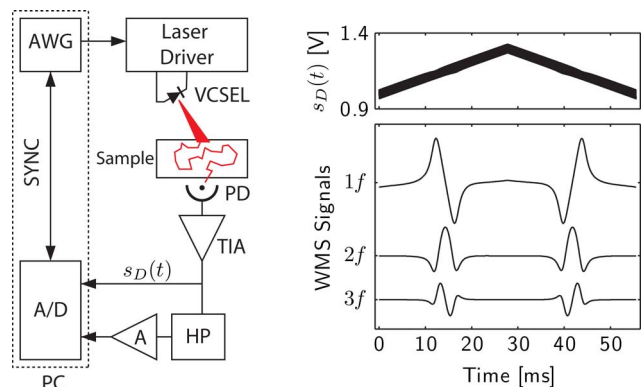


Fig. 1. (Color online) Schematic of the WMS-TDLAS instrumentation, together with sensor and WMS signals (obtained in ambient air measurements).

consists of a triangular ramp (at 18 Hz) that provides a linear frequency sweep and a superimposed harmonic oscillation (18.432 kHz) that allows WMS. In contrast to earlier work, neither optical fibers nor collimating optics are involved. Thus, a divergent beam is injected into our samples (multiple scattering renders collimation superfluous). Light is detected using a $5.6\text{ mm} \times 5.6\text{ mm}$ large-area photodiode (S1337-66BR, Hamamatsu Photonics), and the resulting detector signal is amplified using a low noise transimpedance amplifier (TIA) (DLPCA-200, FEMTO Messtechnik). Data are sampled at 2.4192 MS/s using an analog-to-digital (A/D) board (NI-6132, National Instruments). For improved sensitivity, a high-pass (HP) filtered and amplified (A) version of the detector signal is also sampled. Laser modulation and data acquisition are synchronized, allowing scan averaging and powerful data postprocessing (without the need of lock-in amplification). This approach has been described by Fernholz *et al.* [11]. Although the technique inherently provides multiharmonic WMS detection, all data presented here are based on the second harmonic ($2f$) only. Measurements in ambient air (without a scattering material between laser and detector) show that the system sensitivity is 1×10^{-6} or better (60 s acquisition time). The system is carefully calibrated in ambient air, and obtained WMS signals are later used as absolute references during quantitative analysis of GASMAS data (i.e., curve fitting using a known experimental WMS signal provides the GASMAS L_{eq}). Furthermore, as expected from WMS theory, the intensity-corrected $2f$ WMS peak signal is observed to be ~ 0.3 times the actual absorption fraction [12].

The system performance in GASMAS is characterized by the use of highly scattering, nonporous epoxy samples (10 mm diameter and 3 mm thick) [13]. These samples were manufactured to mimic the optical properties of pharmaceutical solids. By employing photon time-of-flight spectroscopy and diffusion modeling, the reduced scattering coefficient was estimated to $\sim 40\text{ mm}^{-1}$ and the absorption coefficient to $\sim 5 \times 10^{-3}\text{ mm}^{-1}$ (the average optical path length in transmission is of the order of 100 mm). GASMAS measurements on such samples are expected to exhibit oxygen absorption only to the extent of the optical path length offset (space between VCSEL and sample surface). However, even when the path length offset is several millimeters, the registered WMS signal as acquired under static conditions exhibits nothing but a severe optical interference pattern. That the observed signal really is an optical interference pattern is inferred from the symmetry with respect to the triangular scan. Measurements over several minutes reveal that this pattern is stable. However, any small adjustment of either sample or laser position causes a complete change of the interference. This means that mechanical dithering enables us to convert this random (but stable) interference pattern into true interference noise and suppress it by means of waveform averaging.

To quantify interference, the WMS scan was adjusted to place the oxygen absorption imprint in the

edge of our scans (close to the top of the triangular scan). We then use the standard deviation of the interference signal (in the region of no oxygen imprint), I_σ , as a measure of interference level. Figure 2(a) illustrates this procedure, and Figs. 2(b) and 2(c) show how I_σ is influenced by the laser-sample separation. Interestingly, shown in Fig. 2(b), the interference level does not decrease much as the laser is moved further away from the sample. Even when a 75 mm path is added, yielding an absorption fraction of $\sim 2 \times 10^{-3}$ and a WMS peak of 6×10^{-4} , the oxygen imprint is heavily distorted by random interference. If the sample is removed (and replaced by a filter to ensure similar intensity), the I_σ level drops more than 1 order of magnitude. These experiments rule out the possibility that the random interference signal is due to optical feedback into the VCSEL. Instead, it is clear that the observed random interference is due to the sample. The slight increase in I_σ for short distances can possibly be assigned to changes in injection spot size.

The fact that both the utility signal (oxygen absorption) and the limiting random interference signal are generated inside the sample has important implications for the design of GASMAS instrumentation. For example, the dual beam approach used in our previous work on pharmaceutical characterization [10], should not be capable of efficient interference suppression in GASMAS. This is in agreement with our experiences from that work, where we found it essential to impose vibrations to reveal the oxygen imprint.

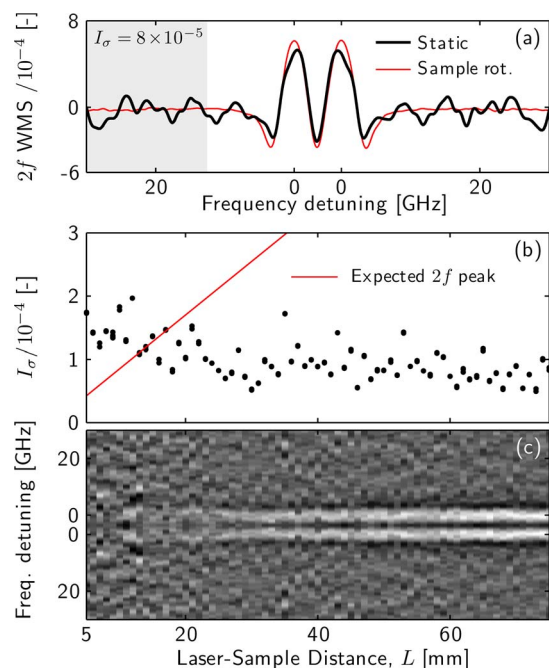


Fig. 2. (Color online) Optical interference encountered in GASMAS is exemplified in (a) (75 mm added path). There, we also show the signal measured with sample rotation (a procedure described below). Influence of the laser-sample distance is presented quantitatively in (b). The increase in the oxygen signal as L is increased is shown in (c), using a free-space oxygen response as reference (right side of image).

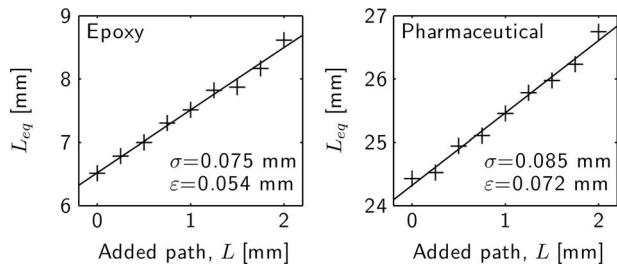


Fig. 3. Sensitivity analysis by means of standard addition and sample rotation. Residual standard deviation σ , and average absolute deviations, ϵ , for linear regression are stated. In epoxy measurements, the obtained signal originates from the ambient air path between laser and sample. Since the same path offset is present in the pharmaceutical data, the oxygen imprint for the tablet is ~ 18 mm L_{eq} .

To overcome the random interference described above, we now propose the use of sample rotation and tracking coils as efficient tools for interference to noise conversion. Tracking coils consists of a lens mounted close to two coils, allowing adjustment of the lens position, and is found in virtually all CD players. If the sample shape renders rotation impossible or inconvenient, this device can be positioned between the laser and the sample. By seeding the coils with appropriate signals, it allows controlled beam dithering as an alternative to sample rotation. Data presented below are acquired using ~ 1 turn/s sample rotations or low frequency (< 100 Hz) feeding of tracking coils.

To measure system performance, we conducted two independent experiments. The first is based on the standard addition technique normally used in chemical analysis (determination of concentrations in unknown samples). It involves adding ambient air path lengths between the laser and the sample and the monitoring of the change in oxygen absorption. The second method involves repeated measurements and calculations of Allan deviation [14]. This experiment was conducted using both the epoxy sample dis-

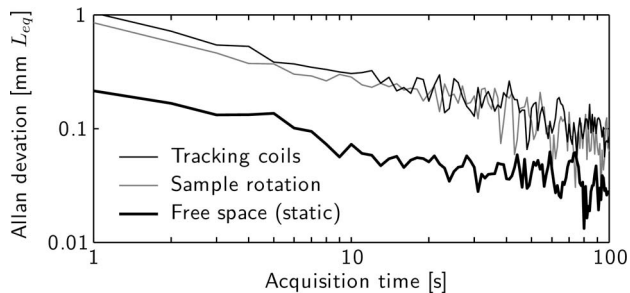


Fig. 4. Allan deviation based on 400 consecutive 1 s measurements. Data shown are from measurements on a pharmaceutical tablet under sample rotation ($L_{eq} = 25.8$ mm), the epoxy sample with tracking coil beam dithering ($L_{eq} = 20.7$ mm), as well from free-space measurements (no scattering sample present, $L_{eq} = 76.5$ mm).

cussed above and the pharmaceutical tablets. The outcome of the standard addition is exemplified in Fig. 3, indicating a sensitivity of ~ 0.1 mm L_{eq} for an acquisition time of 60 s (corresponding to an absorption fraction of 3×10^{-6}). Allan deviations for three measurement cases are shown in Fig. 4. Knowing that the absorption imprint remains hidden if no mechanical dithering is employed, this figure clearly shows the effectiveness of sample rotation and beam dithering.

Utilizing very simple instrumentation, this work clearly demonstrates the first submillimeter GASMAS measurements. Furthermore, repeated measurements on more than ten different pharmaceutical tablets show that the day-to-day reproducibility is ~ 0.3 mm L_{eq} (presumably limited by laser positioning). The high sensitivity in combination with excellent reproducibility and simplistic instrumentation provide both scientific and industrial potential. The use of the proposed approach for characterization of pharmaceutical materials will be described in detail in a forthcoming article [15]

The authors acknowledge the enthusiastic support offered by Sune Svanberg.

References

1. I. Linnerud, P. Kaspersen, and T. Jæger, *Appl. Phys. B* **67**, 297 (1998).
2. P. A. Martin, *Chem. Soc. Rev.* **31**, 201 (2002).
3. P. Kluczynski, J. Gustafsson, Å. Lindberg, and O. Axner, *Spectrochim. Acta, Part B* **56**, 1277 (2001).
4. J. A. Silver, *Appl. Opt.* **31**, 707 (1992).
5. M. Sjöholm, G. Somesfalean, J. Alnis, S. Andersson-Engels, and S. Svanberg, *Opt. Lett.* **26**, 16 (2001).
6. G. Somesfalean, M. Sjöholm, J. Alnis, C. af Klinteberg, S. Andersson-Engels, and S. Svanberg, *Appl. Opt.* **41**, 3538 (2002).
7. M. Andersson, L. Persson, M. Sjöholm, and S. Svanberg, *Opt. Express* **14**, 3641 (2006).
8. L. Persson, H. Gao, M. Sjöholm, and S. Svanberg, *Opt. Lasers Eng.* **44**, 687 (2006).
9. L. Persson, M. Andersson, M. Cassel-Engquist, K. Svanberg, and S. Svanberg, *J. Biomed. Opt.* **12**, 054001 (2007).
10. T. Svensson, L. Persson, M. Andersson, S. Svanberg, S. Andersson-Engels, J. Johansson, and S. Folestad, *Appl. Spectrosc.* **61**, 784 (2007).
11. T. Fernholz, H. Teichert, and V. Ebert, *Appl. Phys. B* **75**, 229 (2002).
12. R. Arndt, *J. Appl. Phys.* **36**, 2522 (1965).
13. M. Firbank and D. T. Delpy, *Phys. Med. Biol.* **38**, 847 (1993).
14. P. Werle, R. Mücke, and F. Slemr, *Appl. Phys. B* **57**, 131 (1993).
15. T. Svensson, M. Andersson, L. Rippe, S. Svanberg, S. Andersson-Engels, J. Johansson, and S. Folestad, "VCSEL-based oxygen spectroscopy for structural analysis of pharmaceutical solids," *Appl. Phys. B* (to be published).